

## Nanostructures

Metallic Nanowires of Nb<sub>3</sub>Te<sub>4</sub>: A Nanostructured Chalcogenide\*\*

Hannah K. Edwards, Pamela A. Salyer, Martin J. Roe,  
Gavin S. Walker, Paul D. Brown,\* and  
Duncan H. Gregory\*

Since the discovery of carbon nanotubes,<sup>[1]</sup> there has been a sharp growth in the research of carbon nanostructures and, latterly, inorganic nanotubes and wires. The promise of a greater breadth of chemical and physical properties from inorganic nanostructures over their carbon counterparts has led to a proactive search for inorganic compounds with the capacity to be synthesized as nanowires or nanotubes. This evolving area of nanomaterials chemistry promises novel

[\*] H. K. Edwards, Dr. P. A. Salyer, Dr. D. H. Gregory

School of Chemistry  
University of Nottingham  
University Park, Nottingham, NG72RD (UK)  
Fax: (+44) 115-951-3563  
E-mail: duncan.gregory@nottingham.ac.uk

H. K. Edwards, M. J. Roe, Dr. G. S. Walker, Dr. P. D. Brown  
School of Mechanical, Materials and Manufacturing Engineering  
University of Nottingham  
University Park, Nottingham, NG72RD (UK)  
Fax: (+44) 115-951-3800  
E-mail: paul.brown@nottingham.ac.uk

[\*\*] D.H.G. thanks the EPSRC for financial support of this work. D.H.G., P.D.B., and G.S.W. thank the IDTC in Nanotechnology at the University of Nottingham for a studentship for H.K.E. The authors also acknowledge use of the EPSRC's Chemical Database (ICSD) service at the Daresbury Laboratory (UK).



Supporting information for this article is available on the WWW under <http://www.angewandte.org> or from the author.

properties through the transition from the bulk phase to the nanoscale and the introduction of additional design elements for materials, such as quantum confinement. The first inorganic nanotubes were synthesized by Tenne<sup>[2]</sup> and many new inorganic nanostructures have been produced since through a small number of increasingly understood synthetic methods.<sup>[3]</sup> By far the largest and most-studied family of these inorganic nanostructures is the transition-metal chalcogenides. This family is dominated by the dichalcogenides  $\text{MX}_2$  ( $\text{M}$  = Group 4–6 metals,  $\text{Re}$ ;  $\text{X}$  = S, Se, Te),<sup>[2–4]</sup> whose component layers of  $\text{MX}_6$  polyhedra, which are separated by van der Waals interactions, are conducive to the rolling or scrolling required for the formation of nanotubes or wires (similar to the “dangling bonds” in graphene layers).<sup>[5]</sup> Only two nanostructured niobium chalcogenides are known,  $\text{NbS}_2$ <sup>[6]</sup> and  $\text{NbSe}_2$ .<sup>[7]</sup> Additionally, nanoscaled  $\text{NbSe}_3$  has also been obtained after being physically cleaved from larger crystals.<sup>[8]</sup> Furthermore, and perhaps surprisingly, only one example of a metal telluride nanomaterial has been reported so far, the dichalcogenide  $\text{MoTe}_2$ .<sup>[9]</sup> Herein, we report the first example of a new class of inorganic nanowire, the telluride  $\text{Nb}_3\text{Te}_4$ . The niobium telluride is unique among the nanostructured chalcogenides in terms of its stoichiometry and, crucially, its structure. In contrast to the dichalcogenides, this 3:4 nanostructured compound is the first to be grown that is derived from a 1D bulk structure. The ensuing electronic properties of such nanowires can be inferred directly from the 1D crystal structure of the material.

Niobium telluride nanowires were synthesized at elevated temperature by direct chemical vapor transport (CVT) from the respective elemental powders in a sealed system (see the Experimental Section). The transition of the starting material from an intimate mixture of powders to nanostructured product was followed (ex situ) by powder X-ray diffraction (PXRD; Figure 1). Elemental Nb and Te react after 1 h at 900 °C to form  $\text{NbTe}_2$  (**1**; Figure 2a), which converts into  $\text{Nb}_3\text{Te}_4$  (**2**) after 1 week. Both the Nb/Te phases are present at the intermediate times of 4 h, 1 day, and 3 days. Material held at 900 °C for 1 h and then annealed at 1160 °C for 2 days also converts from  $\text{NbTe}_2$  into  $\text{Nb}_3\text{Te}_4$  (**3**). Secondary electron (SE) images from scanning electron microscopy (SEM) show well-defined particles for **1** and **2**, as opposed to clusters of nanowires for **3**. Hexagonal lattice parameters of  $a = 10.665(5)$  and  $c = 3.643(2)$  Å were obtained for **3** from PXD data, which were in excellent agreement with previously reported single-crystal data.<sup>[10]</sup> The nanowires grow out from a central core as “sea-urchin-like” clusters (Figure 2b) with lengths of the order of 30 µm. Energy-dispersive X-ray spectroscopy (EDX) analysis yielded an Nb/Te atomic ratio of 43:57 (3:4), which is consistent with  $\text{Nb}_3\text{Te}_4$  and in agreement with the PXD data. Furthermore, back-scattered electron (BSE) imaging indicated a lack of high contrast between the wires, thus suggesting the sample composition to be relatively constant throughout.

X-ray photoelectron spectroscopy (XPS) analysis of **3** yielded a Nb/Te elemental ratio of 0.762:1, again in close agreement with the expected ratio of 0.75:1 for  $\text{Nb}_3\text{Te}_4$ . Furthermore, high-resolution spectra gave binding energies (BEs) of 202.9 and 572.7 eV for the Nb and Te centers in **3**,

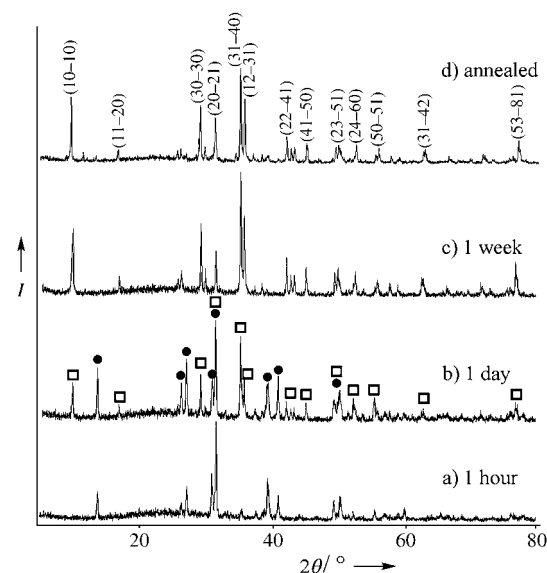


**Figure 1.** XRD patterns of samples sintered at 900 °C after a) 1 h (**1**), b) 24 h, and c) 1 week (**2**) showing the gradual transformation of **1** (solid circles) into **2** (open squares). These samples did not contain nanowires. d) XRD pattern of **1** sintered for 1 h at 900 °C followed by annealing at 1160 °C for 2 days. The resulting sample **3** was composed of clusters of nanowires. (Major peaks are indicated with indices.)

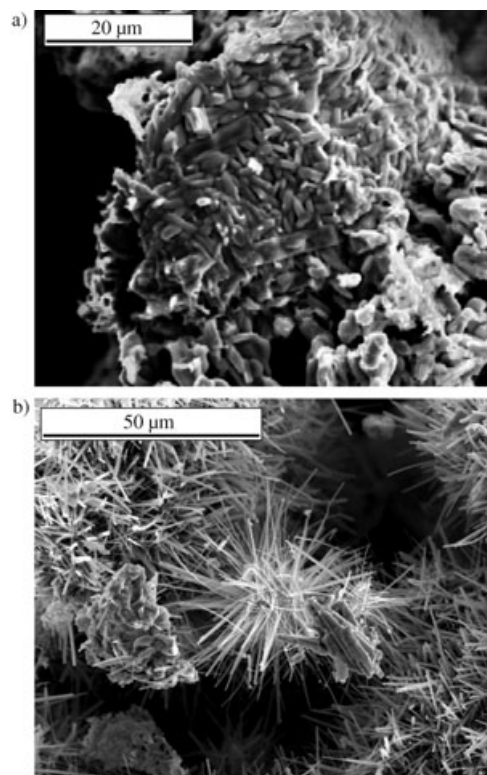


**Figure 2.** SEM micrographs of a)  $\text{NbTe}_2$  particles after 1 h at 900 °C and b) a cluster of  $\text{Nb}_3\text{Te}_4$  nanowires. The nanowires emanate from larger core particles of  $\text{Nb}_3\text{Te}_4$ .

concomitant with BEs in  $\text{Nb}_3\text{Te}_4$  of 202.8 and 572.6 eV, respectively.<sup>[11]</sup> Additional oxide peaks at 206.8 and 576.3 eV were in excellent agreement with the ternary oxides

$\text{Nb}_2\text{Te}_3\text{O}_{11}$  and  $\text{Nb}_2\text{Te}_4\text{O}_{13}$  (where the BEs for the Nb and Te centers are 207.0 and 576.1 eV, respectively),<sup>[12]</sup> thus suggesting some surface oxidation of the telluride that probably occurred during postsynthetic handling. Similar oxide-layer phenomena are observed with nanotubes of  $\text{NbS}_2$ .<sup>[6b]</sup>

Transmission electron microscopy (TEM) analysis revealed the wires are straight with diameters of 50 nm–1  $\mu\text{m}$  (Figure 3). The nanowires exhibit bundled structures, as

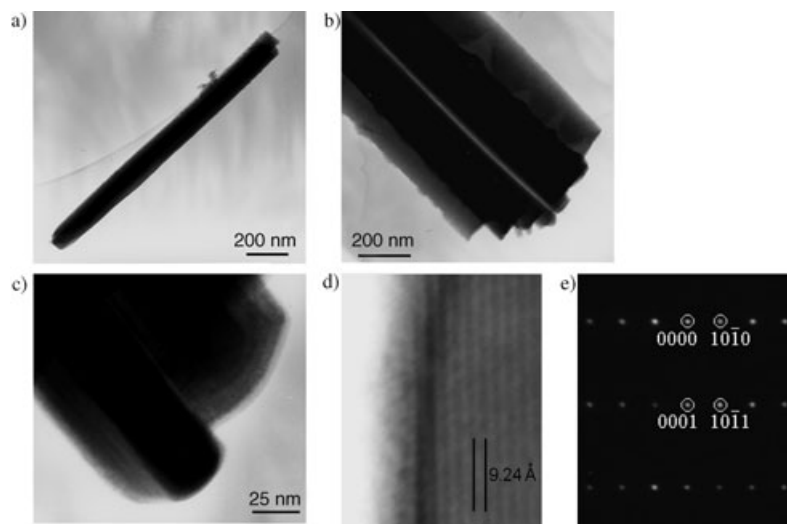


**Figure 3.** TEM images and SAED patterns of the  $\text{Nb}_3\text{Te}_4$  nanowires. a) TEM image of a single nanowire. b) TEM image of bundled nanowires. c) High-magnification TEM image of rounded nanowire ends illustrating the amorphous surface layer found on some wires. (d, e) TEM image and corresponding  $[1-210]$  SAED pattern of the  $(10-10)$  lattice fringes of a  $\text{Nb}_3\text{Te}_4$  nanowire.

if composed of many smaller filaments. Similar bundles are observed with  $\text{NbS}_2$  and  $\text{WS}_2$ , for example,<sup>[6a,13]</sup> although for the telluride, selected-area electron diffraction (SAED) studies confirmed the presence of single crystalline wires, thus suggesting a cooperative growth mechanism. Many wires were found to have rounded ends. The indexing of the nanowire SAED patterns was consistent with the hexagonal  $P6_3/m$  structure of  $\text{Nb}_3\text{Te}_4$ <sup>[10]</sup> and the indexing from PXD. TEM also showed the presence of a thin ( $<5$  nm) surface layer of amorphous material covering the ends and sides of some wires, which is consistent with the surface oxidation indicated by XPS. The combined PXD, XPS, and SAED results indicate that the wires have a  $\text{Nb}_3\text{Te}_4$  core with a surface oxide layer of niobium(v) tellurate. High-resolution electron microscopy (HREM)/SAED revealed that  $\text{Nb}_3\text{Te}_4$  wires grow with the  $[0001]$  direction parallel to the long axis of the wire. The orientation of the  $\text{Nb}_3\text{Te}_4$  planes was also confirmed by measuring the lattice fringes (Figure 3d). The corresponding SAED pattern of projection  $[1-210]$  is shown in Figure 3e, where the plane spacings of 9.24 Å correspond to the  $(10-10)$  (i.e., 100) planes of  $\text{Nb}_3\text{Te}_4$  (9.2414 Å).<sup>[10]</sup> This orientation leads to Nb–Nb chains and open channels running parallel to the long axis of the wire (Figure 4).

Separated wires from **3** display weak, temperature-independent magnetism between 1.8 and 300 K, which is characteristic of a Pauli paramagnet. The bulk material is

reported to be a 1D metal and a superconductor (from electrical resistivity measurements) at approximately 2 K.<sup>[14]</sup> However, no anomaly in the specific heat was observed until 0.5 K and no Meissner effect is seen above 1.4 K.<sup>[15]</sup> Our results for  $\text{Nb}_3\text{Te}_4$  nanowires concur with these earlier findings, thus suggesting that the wires are metallic but not superconducting above 1.8 K.

Although a precise growth mechanism has not yet been established, it is evident from investigating the heating regimes that the annealing process is fundamental to the growth of the nanowires. The elements first react to form  $\text{NbTe}_2$  crystallites, which then transform to  $\text{Nb}_3\text{Te}_4$  nanowires at 1160 °C. Elemental Te has a melting point of 449.5 °C,<sup>[16]</sup> and hence should be molten during the initial reaction step. It is considered that a CVT process subsequently occurs at elevated temperature to yield  $\text{Nb}_3\text{Te}_4$  nanowires from the gas phase which then seed and nucleate outward from an initial core of material. This model is reinforced by SE images showing the characteristic sea-urchin-like form (Figure 2b). SE observations also indicate the formation of hollow-core particles which is consistent with mass transport from the inside to the outside. It is worth noting that transformation from  $\text{NbTe}_2$  to  $\text{Nb}_3\text{Te}_4$  should proceed through the loss of Te, but no Te-containing phases, other than  $\text{Nb}_3\text{Te}_4$ , were detected in the products by PXD. Indexing of the  $\text{NbTe}_2$  phase reveals contraction along the  $c$  axis (i.e., between the Nb–Te layers) relative to the reported parameters,<sup>[17]</sup> thus suggesting that the initial telluride formed is  $\text{Nb}_{1+x}\text{Te}_2$ , by analogy to  $\text{Nb}_{1+x}\text{S}_2$  and, for example,  $\text{V}_{1+x}\text{Te}_2$ .<sup>[18,19]</sup> This ditelluride phase is a subject of our further investigations.

The crystallographic orientation of the wires show that the growth direction is along the hexagonal  $c$  axis.  $\text{Nb}_3\text{Te}_4$  has a large  $a$  value (10.671 Å) and small  $c$  value (3.647 Å). The growth direction of inorganic nanotubes and wires is commonly along that of the shortest lattice parameter.  $\text{Nb}_3\text{Te}_4$  wires are consistent in this respect: they grow with their

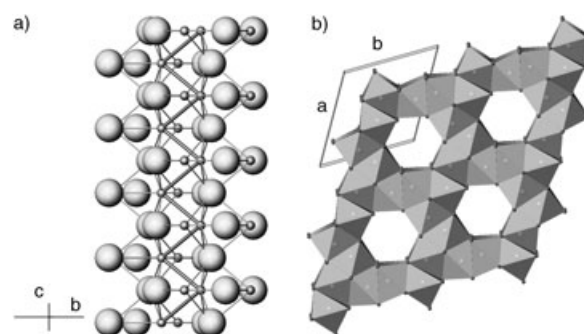


**Figure 4.** a) Crystal structure of  $\text{Nb}_3\text{Te}_4$  to illustrate the Nb–Nb zigzag chains running parallel to the  $c$  axis (small spheres indicate Nb; larger spheres Te) and b) a polyhedral representation in the  $a$ – $b$  plane, which shows the Nb-centred edge-sharing octahedra and open channels that also lie parallel to the  $c$  axis.

[00 $\bar{1}$ ] planes perpendicular to the long axis of the wire. Hence, this growth direction is distinct from chalcogenide nanowires that take a 2D structural basis (smaller  $a$  and larger  $c$  axis).<sup>[2,4]</sup> It is of key importance to the physical properties of the nanowires that the long axis of the wire is also in the same direction as the shortest Nb–Nb bond; infinite zigzag Nb chains run along the  $c$  axis. The intrachain Nb–Nb bond length is 2.973 Å, (Nb metal, Nb–Nb = 2.86 Å),<sup>[20]</sup> whereas the interchain Nb–Nb bond is much longer at 3.854 Å.<sup>[5]</sup> Anisotropic conduction along the  $c$  axis in large single crystals of Nb<sub>3</sub>Te<sub>4</sub> was verified through resistivity and magnetoresistance experiments.<sup>[14b,21]</sup> Nb chains are able to carry charge linearly and are decoupled by the intervening Te atoms. This behavior should be mirrored at the nanoscale, thus inviting compositional and structural modification through substitution (of Te and/or Nb atoms) and intercalation (M<sub>x</sub>Nb(Ta)<sub>3</sub>X<sub>4</sub>); for example, the isostructural Nb<sub>3</sub>S(Se)<sub>4</sub> and intercalates with M = In, Hg, Tl, and Cu, in which  $0 < x \leq 1$ <sup>[22]</sup> are known bulk materials. Hence, there is a real prospect of designing a new family of 1D-derived nanowires exhibiting metallic conduction, charge-density wave phenomena, superconductivity, or fast ionic transport. A systematic study of the growth and properties of such a family is currently underway.

In summary, we have synthesized metallic nanowires of Nb<sub>3</sub>Te<sub>4</sub> for the first time by a high-temperature CVT process. This novel 1D system offers a promising basis for a new family of tailored nanostructured functional materials.

### Experimental Section

Nb<sub>3</sub>Te<sub>4</sub> nanowires were prepared from ground mixtures of niobium (99.9%, Aldrich) and tellurium powders (99.99%, Alfa; molar ratio = 3:4) in a nitrogen-filled recirculating glove box. The mixtures were initially heated in evacuated (approximately 10<sup>−3</sup> mbar) 12-mm diameter sealed silica ampoules to 900 °C for between 1 h and 1 week. After quenching the ampoules in air, the ampoules were subsequently annealed at 1160 °C for 2 days. The resulting low-density black powder was characterized by PXD (Philips X'Pert  $\theta$ -2 $\theta$  diffractometer; Cu<sub>K $\alpha$</sub>  radiation), SEM (JEOL 6400 SEM with an Oxford Instruments ISIS EDX system), XPS (VG Scientific Escalab Mark II spectrometer using Al<sub>K $\alpha$</sub>  radiation at an anode potential of 10 kV and a filament emission current of 20 mA), and TEM (JEOL 2000fx TEM with an ISIS EDX system) for nanoscale imaging and SAED studies. Samples for analysis by SEM and XPS were prepared by depositing powder on to a carbon tab of sufficient thickness to prevent detection of the underlying carbon. Samples for TEM analysis were prepared by sonicating the powders in acetone for 3 min and then transferring drops of the suspension by pipette onto holey carbon-film Cu grids. Samples for SQUID (superconducting quantum interference device) analysis were prepared in similar a manner to separate the nanowires from any residual powder and were then loaded into gelatine capsules. Magnetic measurements were performed using a quantum design MPMS 5T SQUID susceptometer under a field of 1 Oe between 1.8 and 300 K.

Received: January 14, 2005

Published online: April 29, 2005

**Keywords:** chalcogenides · chemical vapor transport · nanostructures · niobium · tellurium

- [1] S. Iijima, *Nature* **1991**, 354, 56.
- [2] R. Tenne, *Nature* **1992**, 360, 444.
- [3] a) C. N. R. Rao, F. L. Deepak, G. Gundiah, A. Govindaraj, *Prog. Solid State Chem.* **2003**, 31, 5; b) M. Remškar, *Adv. Mater.* **2004**, 16, 1497.
- [4] For example: a) V. V. Ivanovskaya, G. Seifert, *Solid State Commun.* **2004**, 130, 175; b) M. Nath, C. N. R. Rao, *Angew. Chem.* **2002**, 114, 3601; *Angew. Chem. Int. Ed.* **2002**, 41, 3451; c) M. Nath, C. N. R. Rao, *Pure Appl. Chem.* **2002**, 74, 1545; d) Y. Feldman, *Science* **1995**, 267, 222; e) R. Harpeness, A. Gedanken, A. M. Weiss, M. A. Slifkin, *J. Mater. Chem.* **2003**, 13, 2603.
- [5] a) R. Tenne, *Chem. Eur. J.* **2002**, 8, 5297; C. N. R. Rao, M. Nath, *Dalton Trans.* **2003**, 1.
- [6] a) X. Wu, Y. Tao, X. Ke, J. Zhu, J. Hong, *Mater. Res. Bull.* **2004**, 39, 901; b) Y. Z. Jin, W. K. Hsu, Y. L. Chueh, L. J. Chou, Y. Q. Zhu, K. Brigatti, H. R. Kroto, D. R. M., Walton, *Angew. Chem.* **2004**, 116, 5788; *Angew. Chem. Int. Ed.* **2004**, 43, 5670; c) C. Schuffenhauer, R. Popovitz-Biro, R. Tenne, *J. Mater. Chem.* **2002**, 12, 1587; d) G. Seifert, M. Terrones, M. Terrones, T. Frauenheim, *Solid State Commun.* **2000**, 115, 635; e) M. Remskar, A. Mrzel, A. Jesih, F. Levy, *Adv. Mater.* **2002**, 14, 680.
- [7] a) T. Tsuneta, T. Toshima, K. Inagaki, T. Shibayama, S. Tanda, S. Uji, M. Ahlskog, P. Hakonen, M. Paalanen, *Curr. Appl. Phys.* **2003**, 3, 473; b) M. Nath, S. Kar, A. K. Raychaudhuri, C. N. R. Rao, *Chem. Phys. Lett.* **2003**, 368, 690.
- [8] E. Slot, M. A. Holst, H. S. J. van der Zant, S. V. Zaitsev-Zotov, *Phys. Rev. Lett.*, **2004**, 93, 176602.
- [9] L. H. Qiu, V. G. Pol, Y. Wei, A. Gedanken, *J. Mater. Chem.* **2003**, 13, 2985.
- [10] K. Selte, A. Kjekshus, *Acta Crystallogr.* **1964**, 17, 1568.
- [11] J. F. Moulder, W. F. Stickle, P. E. Sobol, K. D. Bomben, *Handbook of X-Ray Photoelectron Spectroscopy*, Physical Electronics, Minnesota, **1992**.
- [12] F. Garbassi, J. C. J. Bart, G. Petrini, *J. Electron Spectrosc. Relat. Phenom.* **1981**, 22, 95.
- [13] M. Remškar, Z. Škraba, M. Regula, C. Ballif, R. Samjinés, F. Lévy, *Adv. Mater.* **1998**, 10, 246.
- [14] a) E. Amberger, K. Polborn, P. Grimm, M. Dietrich, B. Obst, *Solid State Commun.* **1978**, 26, 943; b) Y. Ishihara, I. Nakada, *Solid State Commun.* **1983**, 45, 129; c) Y. Ishihara, I. Nakada, *Jpn. J. Appl. Phys.* **1984**, 23, 851.
- [15] H. Okamoto, H. Taniguti, Y. Ishihara, *Phys. Rev. B* **1996**, 53, 384.
- [16] *Handbook of Chemistry and Physics*, 61st ed. (Ed.: R. C. Weast), CRC, Boca Raton, FL, **1980**, p. B154.
- [17] B. E. Brown, *Acta Crystallogr.* **1966**, 20, 264.
- [18] a) F. Jellinek, G. Brauer, H. Mueller, *Nature* **1960**, 185, 376; b) B. Morosin, *Acta Crystallogr. Sect. B* **1974**, 30, 551; c) D. R. Powell, R. A. Jacobson, *J. Solid State Chem.* **1981**, 37, 140.
- [19] K. D. Bronsema, G. W. Bus, G. A. Wiegers, *J. Solid State Chem.* **1984**, 53, 415.
- [20] J. W. Edwards, R. Speiser, H. L. Johnston, *J. Appl. Phys.* **1951**, 22, 424.
- [21] Y. Ishihara, I. Nakada, *Jpn. J. Appl. Phys.* **1984**, 23, 85.
- [22] a) O. Hiroyuki, K. Takuya, G. Muramoto, I. Yoshiaka, S. Yuusuke, M. Iori, K. Hiroshi, I. Yuake, *Phys. B* **2003**, 329, 1350; b) T. Ohtani, A. Tsubota, K. Ohshima, *Mater. Res. Bull.* **1999**, 34, 1143; T. Ohtani, Y. Sano, Y. Yokota, *J. Solid State Chem.* **1993**, 103, 504.